

# Implementation of a pulsed-laser measurement system in the National Transonic Facility

Daniel T. Reese,<sup>1</sup> and Ross A. Burns<sup>2</sup>  
*National Institute of Aerospace, Hampton, VA 23666, United States*

Paul M. Danehy,<sup>3</sup> and Eric L. Walker<sup>4</sup>  
*NASA Langley Research Center, Hampton, VA 23681, United States*

and  
William K. Goad<sup>5</sup>  
*Jacobs Technology, Inc., Hampton, VA 23666, United States*

**A remotely-adjustable laser transmission and imaging system has been developed for use in a high-pressure, cryogenic wind tunnel. Implementation in the National Transonic Facility has proven the system suitable for velocity and signal lifetime measurements over a range of operating conditions. The measurement system allows for the delivery of high-powered laser pulses through the outer pressure shell and into the test section interior from a mezzanine where the laser is free from environmental disturbances (such as vibrations and excessive condensation) associated with operation of the wind tunnel. Femtosecond laser electronic excitation tagging (FLEET) was utilized to provide freestream velocity measurements, and first results show typical data that may be obtained using the system herein described.**

## I. Introduction

Wind tunnel testing at flight-accurate Reynolds numbers is of vital importance to the continued progress of aerospace vehicle research and development. Matching the large Reynolds numbers experienced in flight using small-scale wind tunnel models requires high pressures and low temperatures, as well as sonic velocities. Operating this way leads to both a complex testing environment and a large, multi-discipline facility, making the implementation of optical diagnostics difficult. In the National Transonic Facility (NTF), the feasibility of Rayleigh scattering flow diagnostics was explored by employing Rayleigh and Mie scattering using a fiber optic laser system present in the facility [1]. Rayleigh light scattering was found to be viable as a quantitative diagnostic to measure flow density, while Mie scattering measurements provided estimates of the free-stream particle flux in NTF, which was shown to be dependent on the model angle of attack. Pressure sensitive paint has also been employed to measure global surface pressures on a model [2]. Photogrammetry is routinely used in NTF to measure wing deformation [3]. In reference [3], induced wing twist and deflection from aerodynamic loading were measured at five spanwise locations, and showed that both wings had more induced wing twist at low values of lift coefficient than expected. Measurements of flow disturbance in the NTF were taken using a survey rake containing various temperature, velocity, and pressure probes [4]. The cryogenic mode was found to be a harsh environment, negatively impacting the survivability and repair of hot wire probes, while substantial spatial variation of the unsteady disturbance field was measured for the air mode.

Despite the various techniques employed thus far in the NTF, none have measured the freestream flow velocity non-intrusively. The present work describes the first off-body velocity measurements in NTF using the femtosecond laser electronic excitation tagging (FLEET) technique. FLEET works by focusing a femtosecond laser to dissociate/ionize molecular nitrogen [5]. Photons released during recombination allow the tagged region of fluid to act as a long-lifetime tracer that then advects downstream with the flow and can be tracked through sequential imaging.

---

<sup>1</sup> Research Engineer, AIAA Member

<sup>2</sup> Research Engineer

<sup>3</sup> Senior Technologist for Advanced Measurement Systems, AIAA Associate Fellow

<sup>4</sup> Chief Engineer for Test Operation Excellence, AIAA Associate Fellow

<sup>5</sup> Technical Specialist, ASCET

Previous experiments by Burns et al. have proven FLEET to provide velocity measurements in a transonic, cryogenic environment using the NASA Langley Research Center’s 0.3-m TCT [6,7], as well as demonstrated the ability of the technique to make velocity measurements around a transonic airfoil [8].

In order to carry out the laser-based measurements described in the present work, an integrated and remotely-controlled system consisting of a variety of interplaying subsystems was developed to deliver a femtosecond laser pulse to the center of the NTF test section and image the resultant signals. An overview of the experimental facility is given in the following section. The various subsystems required to provide these measurements are described in further detail in Section III. Preliminary experimental results obtained in this study are discussed in Section IV. Section V covers future work that may be undertaken making use of the modifications described in this report, and Section VI summarizes the conclusions reached regarding the implementation of femtosecond-laser-based optical measurements in the NTF.

## II. Experimental Facility

The NTF is a fan-driven, closed-circuit, cryogenic wind tunnel that uses cryogenic nitrogen gas at high pressure to duplicate true flight aerodynamics [9]. Though nitrogen is used to achieve the lowest temperatures (116 K), the tunnel can also be run using dry air and is capable of reaching temperatures up to 340 K. The wind tunnel has a double-walled construction, with an outer shell used to contain the high pressures experienced during testing (up to 860 kPa), and an inner test section with slotted walls that serves as the channel through which the test gas flows [10]. The test section is 2.5 m by 2.5 m and 7.62 m long, and supports flow within a Mach number range of approximately 0.1 to 1.2. Existing optical access is limited to several windows embedded in the test section walls, ceiling, and floor. The facility has existing surveillance capabilities as well as a data acquisition system (DAS) that allows for acquiring, processing, recording, and displaying of test data.

This report focuses on modifications that have been made to the NTF wind tunnel that will ultimately allow for the application of many different pulsed-laser measurements systems. While FLEET is used as a demonstration of this new capability, it should be noted that the system discussed in the present work is not exclusively designed for — or limited to — application of the FLEET technique. Rather, as designed, the system can be used for most common laser-based measurement techniques, pending operability. The laser delivery system introduced in Section III.A allows for a variety of pulsed and continuous-wave laser systems to deliver light to the facility. By making slight modifications to the laser penetration system discussed in Section III.B, for example replacing optical components such as windows and mirrors, the system as described in this report can be adapted to accommodate most common laser wavelengths without significant redesign. Additionally, simple adjustments such as increasing or decreasing pipe lengths would allow for measurements at various locations within the wind tunnel test section. Likewise, the camera enclosure detailed in Section III.C can be moved to view other regions of the test section, and components can be easily replaced or added, provided there is sufficient space for the equipment. Finally, the control system outlined in Section III.D is adaptable, allowing for the addition or removal of subsystems as required by the applied diagnostic technique.

The experimental campaign outlined in this report was conducted simultaneously with a survey rake test similar to that carried out previously by King et al. [4]. Though not a permanent fixture of NTF, from the perspective of the FLEET experiment, this rake model was considered part of the experimental facility. The survey rake spanned 2.1 m with a chord length of 28.9 cm and maximum thickness of 24 mm. The rake has a double wedge airfoil shape, mounts to the wind tunnel model support structure, and has 21 ports for mounting probes with a 10.16 cm centerline-to-centerline spacing. Throughout the test, the survey rake would be rotated in six-degree increments to allow for pressure, temperature, and velocity measurements along the tunnel cross section. Due to the high power of the femtosecond laser and the potential for model damage, the location of the FLEET focal point relative to the proximity of to the probes was carefully considered, and placed several inches upstream of the survey rake probes. Additionally, to prevent the detection of potential disturbances in the flow caused by the FLEET signal, FLEET data were only taken after the survey rake had completed data collection.

## III. Experimental Setup

Each subsystem (and its interaction with the other subsystems) is described in this section. These subsystems include the laser delivery system, the laser penetration system, an environmentally-controlled vessel for sensitive electrical and optical components (referred to as the “camera enclosure”), and the unifying control system.

### A. Laser Delivery System

A regeneratively-amplified, Ti:Sapphire laser system (Spectra-Physics Solstice) with a repetition rate of 1 kHz, temporal bandwidth of 70 fs, center wavelength of 800 nm, and bandwidth of 13 nm was used to write the FLEET

line. If another laser-based measurement technique were to be applied, most pulsed lasers could be put in the same position, and evacuated or nitrogen-purged beam tubes could be put in place should the diagnostics demand it (e.g., for excimer lasers). The laser was placed in a curtained, laser-safe area on a mezzanine located nearly at the same height as the top of the tunnel but located about 10 meters away from the tunnel so as to be free from environmental disturbances associated with operation of the wind tunnel, such as vibrations and excessive condensation. The laser area had collinear femtosecond and eye-safe alignment lasers, and an optical shutter only allowed passage of the laser beam while acquiring velocity measurements. To adjust laser power from the control room, a remotely-controlled attenuator was placed just downstream of the optical shutter. Using a two-lens Galilean telescope near the laser, the laser beam diameter was increased to enable a tighter focus in the test section and to help prevent damage to the downstream optics. A periscope system was used to bring the laser beam to the same height as the entry to the laser penetration system and to deliver the laser from the mezzanine to the facility. The final mirror of the periscope was motorized and mounted on a remotely-controlled translation stage in order to compensate for the tunnel expansion and contraction that occurs as run temperatures were changed. An image showing the curtained, laser-safe area on the mezzanine in relation to the wind tunnel is given in Fig. 1(a). Also in Fig. 1(a) is the beam path (shown as a dashed red line) spanning the gap from the exit of the periscope in the laser delivery system to the entrance of the laser penetration system mounted on top of the wind tunnel. A detail showing the beam entering the laser penetration system is given in the lower left corner of Fig. 1(a), which is also the top left of Fig. 1(b). The flange shown below corner housing #1 in this detail mounts to the outer pressure shell and separates the outside of the wind tunnel from the high pressure environment inside the plenum.

## B. Laser Penetration System

The transmission optics and associated control systems used to deliver the laser beam through the high pressure shell, through the plenum, and into the test section are known as the laser penetration system (LPS). The LPS consists of four sections of 5 cm diameter stainless steel tube joined by three mirror housings. An image of the LPS (wrapped in heating tape) within the plenum section of NTF is shown in Fig. 1(b), where the mirror housings are circled in yellow and the beam path within the LPS is shown as a dashed red line. Windows were mounted on the ends of the tubes so that a vacuum could be pulled within the LPS, allowing for the laser to pass through the NTF plenum without beam quality being degraded by the high density environment. The mirror housings each contain a remotely adjustable mirror and a small video camera; one such housing is shown in the corner housing detail inset of Fig. 1(b). A video feed indicating the position of the laser beam on each mirror was monitored from the facility control room where each of the mirrors were adjusted to ensure transmission of the light into the facility; this beam monitoring system is shown in Fig. 1(c) where the view of all cameras in each of the three LPS mirror housings show the beam location on each mirror as a bright white circle while the mirror edge is visible as a faint white ring surrounding each circle. As aligned in Fig. 1(c), the beam is well centered on the first two mirrors (as indicated by the single bright circle centered on the mirror in the top two frames) but misaligned on the third mirror (indicated by the presence of more than one bright spot, neither of which are centered on the mirror). This misalignment would be remedied by using the motorized mirror in the second mirror housing to drive the beam to the center of mirror number three.

Once centered on all three mirrors within the LPS, the final mirror was used to drive the beam through a focusing lens telescope and a turning prism assembly attached to the end of the LPS. A schematic of this optical assembly is shown in Fig. 2(a). As the beam exited the final window of the LPS, it first passed through a 50 mm diameter UV grade fused silica -300 mm plano-concave lens in order to expand the beam; this larger beam diameter allowed the beam to ultimately focus tighter inside the NTF test section. The focusing of the beam was accomplished using a 50 mm diameter UV grade fused silica +400 mm focal length plano-convex lens. Downstream of the focusing optic, the laser passed through a wedge prism. Because the windows in the ceiling of the test section (used for passage of the laser beam) are not aligned with the windows on the side walls of the test section (used for imaging the FLEET signal), the wedge prism was necessary in order to direct the beam upstream to a location within view of the camera. However, the turning prism was detrimental to the FLEET signal, cutting the signal intensity detected by the camera nearly in half compared to not using the prism. After the light exited the turning prism, it was directed through a window in the test section ceiling and into the facility where it was focused near the tunnel centerline. The beam path as seen from inside the test section is shown in Fig. 2(b), where the beam path is indicated by a red line, the camera field of view is shown as a blue rectangle, and the survey rake can be seen downstream of the camera field of view. It is important to note that, should a different laser-based measurement technique be applied, all of the optical elements in the laser penetration system (such as mirrors and windows) could be adapted to accommodate most common laser wavelengths without significant redesign. Additionally, the optical assembly attached to the end of the LPS could easily be designed to include different (or additional) lenses and wedges, or be removed altogether.

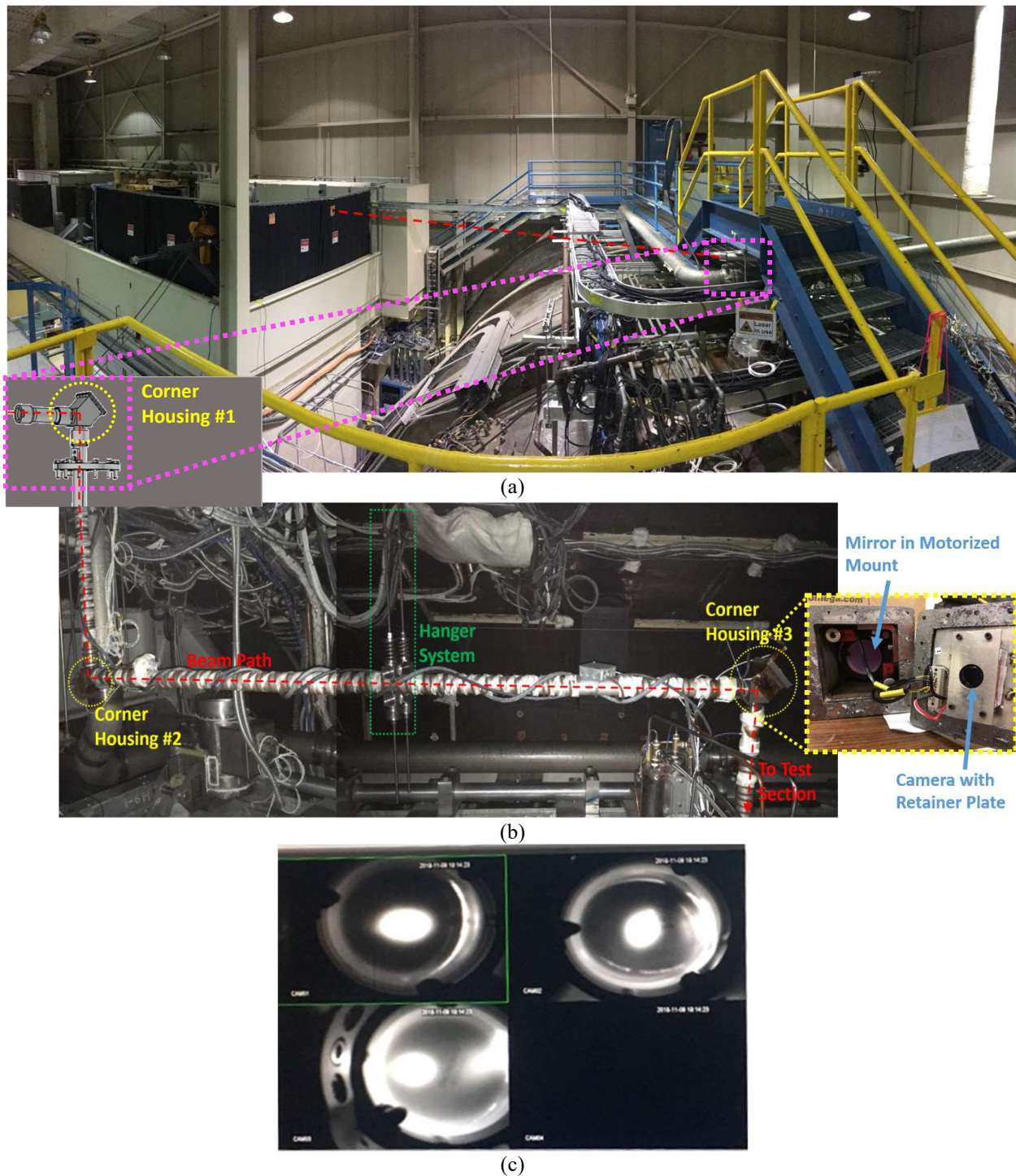


**Figure 1. Laser penetration hardware and control.** (a) Laser beam path from curtained, laser-safe area on mezzanine to the entrance of the LPS shown as a dashed red line. (b) Portion of LPS inside the plenum used to deliver the beam from outside the wind tunnel to the center of the test section. A hanger system used to support the weight of the LPS is outlined in green, while corner housings are circled in yellow and the beam path is shown as a dashed red line. (c) Video surveillance system used to track and steer the beam into the test section.

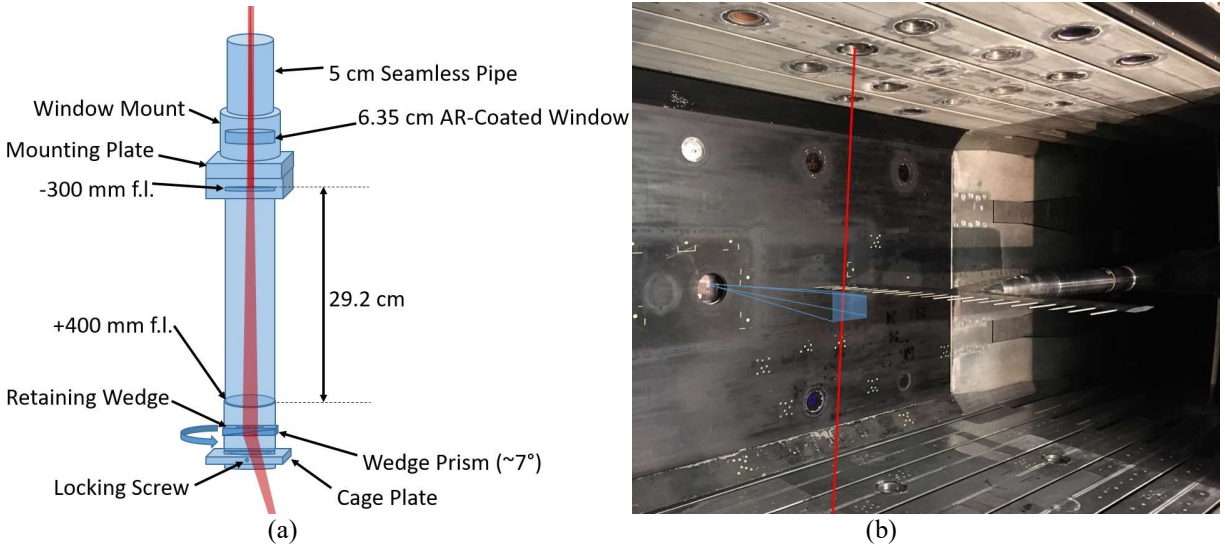


**Figure 2. Optical assembly and test section of the NTF configured for the current studies.** (a) Schematic of the optical assembly, including telescope and turning prism, shown attached to the end of the LPS. (b) Test section of the NTF. The red line indicates the laser passing through the window in the top of the test section, while the blue rectangle represents the field of view of the camera housed in the test section side wall.

### C. Camera Enclosure

Imaging of the FLEET signal was done using a high-speed image intensifier (LaVision HS-IRO) lens-coupled to a CMOS camera (Photron Mini AX-200) with an objective lens (Canon EF 135mm f/2). The focus and aperture of the objective lens had the capability to be remotely-adjusted; however, this feature was not utilized during this experimental campaign as the FLEET signal was held at a fixed position throughout the duration of the test. The camera frame rate was 1 kHz (matching the laser) so that each frame contained FLEET signal from a single laser pulse. To capture multiple delayed exposures of the FLEET signal on a single frame, the intensifier was gated ten times using a gate width of 4 microseconds with 10 microseconds between gates. The imaging system was mounted halfway up the test section wall inside of the plenum section and viewed the FLEET signal through a 20.3 cm diameter fused silica window, as shown in Fig. 2(b). Because this area is subject to the high pressure and low temperature environment present during tunnel operation, the intensified, high-speed camera system was placed inside of a temperature- and pressure-controlled camera enclosure. Heating was provided by electrical heaters while cooling was provided by cool purge air (during air mode operation). The enclosure is cylindrical in shape. The interior measures approximately 74 cm long by 33.5 cm in diameter. This camera enclosure also contained a network switch for communicating with the various components, and a filter wheel that allowed different optical filters to be placed in front of the objective lens. The entire imaging system and camera enclosure could be moved around to other windows, if necessary, and could accommodate many different cameras, intensifiers, and additional components, subject to the size constraints of the enclosure; this ensures that the system is versatile enough to handle most common laser diagnostics, not just the FLEET system used in the current studies. The temperature and pressure in the camera can be monitored remotely, and the pressure was maintained between 101 kPa and 152 kPa while the temperature stayed in a range between 289 K and 326 K.

### D. Control System

All subsystems described above are controllable remotely from both the mezzanine and the control room via a local Ethernet network. This setup allowed every computer in the network the ability to select the laser power, monitor and steer the beam through the LPS, control all camera and intensifier settings, adjust the objective lens focus and aperture, and select the desired imaging filter. Additional computers can be easily integrated into the network by running an Ethernet cable to an open port in an existing network switch; this feature was utilized, for example, in order to adjust laser and camera settings from within the test section during experimental setup taking place prior to the test.



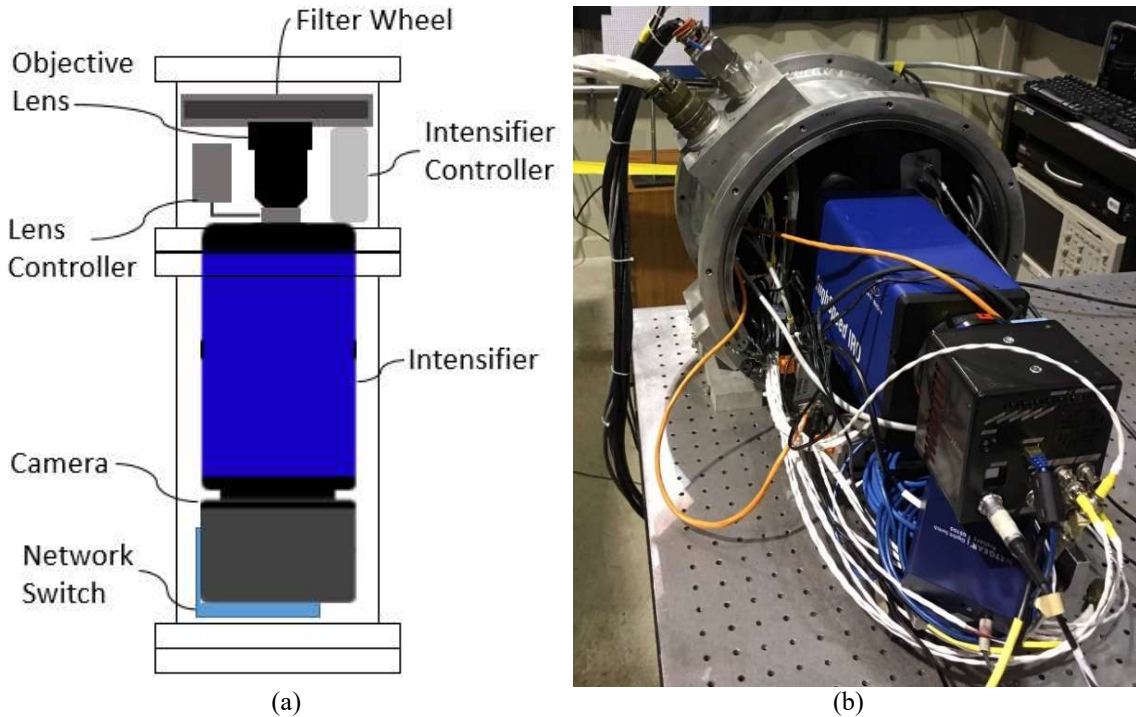


**Figure 3. Camera enclosure.** (a) Schematic showing the placement of various components within the camera enclosure. (b) Photograph of the camera enclosure without backmost portion of the containment shell.

#### IV. Experimental Results

The modifications that were made to the NTF will ultimately allow for the application of many different laser measurement techniques. Here we discuss two main experimental results that were obtained through the application of FLEET using the experimental setup described in the previous section: unseeded velocimetry, and FLEET signal lifetime measurements at various facility testing conditions. FLEET signal lifetimes are relevant because they impact the accuracy and precision of FLEET velocimetry. Results were obtained in both air and nitrogen environments, at temperatures ranging from 172 K to 322 K, pressures from 138 kPa to 827 kPa, and Mach numbers from 0.2 to 0.95; though only preliminary results from a single condition are presented in this report. Subsection A discusses the velocity measurements made using the pulsed-laser measurement system in NTF, while Subsection B presents FLEET signal lifetime measurements. The data shown here is preliminary, and is meant to be indicative of the type of data that can be collected using the pulsed-laser measurement system introduced in this report.

##### A. Velocimetry

FLEET signal images are captured as the tagged molecules advect downstream towards the survey rake. Preliminary data and analysis are shown in Fig. 4 for nitrogen at Mach 0.8,  $T=278$  K, and  $P=207$  kPa. An average of raw FLEET images is shown in Fig. 4(a) with a magnified region of interest around the FLEET signal more clearly showing the angle of the signal caused by the turning prism. In this image, which is comprised of multiple exposures captured on a single frame by exposing the camera over several intensifier gates, the initial FLEET signal is shown as a bright line that moves rightward with the freestream flow. Subsequent exposures of the FLEET line show intensity decay as time progresses. To obtain velocity, raw images are first rotated to align FLEET signal with the vertical as shown in Fig. 4(b).

Signal intensity profiles, as shown by dots in Fig. 4(c), are obtained from a region of interest cropped from the rotated data by integrating the FLEET signal along the vertical direction. By first smoothing the profile using a moving average, a peak-finding algorithm can then be used to determine the number of exposures containing FLEET signal above a given noise floor value. The approximate peak intensities and locations of the peaks determined from the smoothed profile are shown as open-faced triangles in Fig. 4(c), while the noise floor is shown as a dashed line. To

obtain the actual peak intensity and location of each FLEET line to sub-pixel accuracy, FLEET profiles are modeled as a series of Gaussians on a ramp as,

$$I = \alpha + \beta x + \sum_{k=1}^n \gamma_k e^{\frac{-(x-\delta_k)^2}{\epsilon_k}}, \quad (1)$$

where  $\alpha, \beta, \gamma, \delta,$  and  $\epsilon$  are fit parameters, and  $n$  is determined by the number of exposures containing FLEET signal on the frame of interest. This model is shown fit to data in Fig. 4(c) as a solid red line containing six peaks; typical FLEET data contained four to six peaks, depending on the flow conditions. Peak intensities and locations are then determined to sub-pixel accuracy by finding peaks of the fit model, and are shown in Fig. 4(c) as black diamonds. The slope of a linear fit to the peak positions in time (i.e.  $x$  vs.  $t$ ) is then used to estimate velocity as shown in Fig. 4(d). The streamwise component of velocity is then calculated using the rotation angle determined in step one of data processing.

## B. Lifetime Measurements

In addition to the peak signal positions extracted for use in velocimetry, information on the FLEET signal lifetime can be determined from the model fit to data. The FLEET signal lifetime has important implications for the uncertainty of velocity measurements, with longer lifetimes generally correlating with more precise results. To determine the signal lifetime, peak intensity decay is fit as a function of time using a bi-exponential model,

$$I(t) = ae^{bt} + ce^{dt}. \quad (2)$$

The signal lifetime ( $\tau$ ) can then be defined to be the time that the signal reaches  $1/e$  of the initial value. Figure 4(e) shows the measured peak intensity as black diamonds, the bi-exponential model fit to data as a solid line, and the measured lifetime as a star. It should be noted that, although the results shown in Fig. 4 are for averaged signal across the measurement time, preliminary studies show that single-shot velocity can be obtained, with the retention of spatial resolution along the 2.5 cm long excited line under certain tunnel operating conditions.

## V. Future Work

The modifications to NTF described in the present work provide the opportunity for many future experiments utilizing pulsed-laser diagnostics. Though the work described in this report details the application of FLEET velocimetry in freestream flow as a proof-of-concept experiment, the potential for similar velocimetry measurements on a model to measure flow separation, velocity deficits, or even vorticity exists; in fact, a campaign using FLEET to measure the flow velocity in a region behind the wing of the common research model (CRM) is currently underway. In addition to velocimetry measurements, the measurement system as described above is capable of making density measurements through application of Rayleigh scattering without requiring any modifications outside of changes to the intensifier gate timing and camera filters used (which are controlled remotely). By making very minor changes to the laser delivery system and LPS (i.e. changing windows, mirrors, and the optics assembly attached to the LPS), a pulse-burst laser [11-13] can be used in place of the current femtosecond laser. This pulse-burst laser system would allow for a variety of time-resolved measurements including Doppler global velocimetry (DGV), particle image velocimetry (PIV) [14] or particle tracking velocimetry (PTV), picosecond laser electronic excitation tagging (PLEET) [15], filtered Rayleigh scattering (FRS), and Rayleigh scattering density (RSD). The system described in Section IV can be adapted to accommodate nearly any pulsed-laser measurement technique that can be applied in the NTF.

In addition to opening the door to a number of other pulsed-laser measurement techniques, incremental improvements can be made to the current system to allow for better FLEET velocity measurements. For example, by removing the turning prism in the optics assembly attached to the LPS, a factor of two signal can be recovered, thus increasing the signal-to-noise obtained in the current experiments. Because the FLEET signal would still need to be directed in front of the camera's field of view, a pair of mirrors can be used to direct the beam with more control than is currently available using the turning prism. This option was not taken for the current experiment due to time constraints dictating the use of the turning prism. It is also possible that the second mirror in this turning-mirror-pair be motorized, allowing for remote movement of the FLEET signal within the test section, thereby allowing two-dimensional velocity measurements.

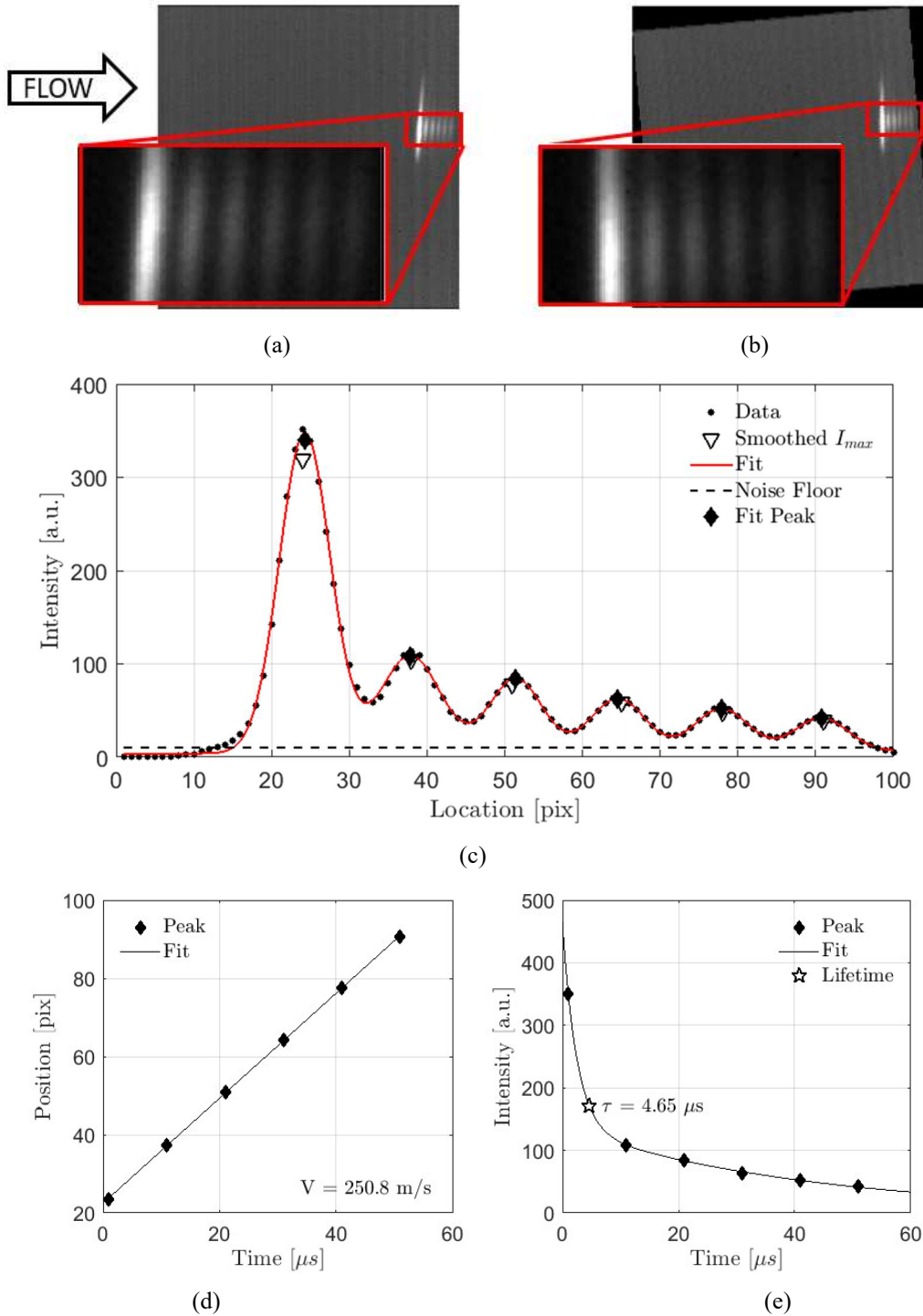


**Figure 4. Representative average FLEET velocity and signal lifetime measurements for  $N_2$ .** (a) Averaged, full-frame FLEET signal and region of interest (ROI). (b) Signal rotated to align FLEET line with the vertical, and corresponding ROI used for further analysis. (c) Mean intensity profile for rotated ROI is shown as dots and a model fit is shown as a solid red line. (d) Peak position as a function of time and linear fit used to determine velocity. (e) Peak intensity as a function of time, with bi-exponential fit (solid line) and signal lifetime marked by a star.



## VI. Conclusions

An implementation of pulsed-laser diagnostics was carried out successfully in the NTF to allow for FLEET velocimetry and signal lifetime measurements over a range of operating conditions. This was accomplished through the integration of several subsystems which allowed for the delivery and detection of a femtosecond laser to the center of the test section and the resultant signal. A laser delivery system provided the ability to remotely adjust laser power and deliver the light from a laser-safe area to the laser penetration system mounted on the tunnel. The system allows for adjustments required to accommodate the expansion and contraction of the wind tunnel at various operating temperatures. A remotely-monitored and adjustable laser penetration system provided an evacuated beam path from outside of the wind tunnel, through the high density gas inside the plenum, and into the test section. The LPS also had a series of optics to focus and direct the laser beam in the field of view of the camera. A camera enclosure maintained the temperatures and pressures required for the safe operation of an intensified camera system, with the ability to remotely select various optical filters, objective lens focus and aperture, as well as all camera and intensifier settings. Results were obtained in both air and nitrogen environments, at temperatures ranging from 172 K to 322 K, pressures from 138 kPa to 827 kPa, and Mach numbers from 0.2 to 0.95. While only a single example of raw data is shown in this paper, a more detailed analysis of the performance of this system is forthcoming. Though the pulsed-laser measurement system described in this report was proven in freestream conditions using the FLEET technique, this is a versatile system that will ultimately allow for a variety of measurements using a number of different laser measurement techniques.

## Acknowledgments

We wish to recognize the contribution of Peyton Gregory for his help in designing the laser penetration system. We also wish to thank the entire NTF staff for their help setting up the laser-safe area on the mezzanine, the camera enclosure, and the laser penetration system as well as the operation of the facility. We would like to acknowledge Chloe Dedic (University of Virginia) for contributions to the experimental setup, and Josef Felver, Naibo Jiang, and Sukesh Roy (Spectral Energies) for their assistance with the laser and penetration system software. This work was supported by NASA's Aerosciences Evaluation and Test Capabilities (AETC) Portfolio under the leadership of Ron Colantonio and James Bell, lead for Test Technology. Funding for this project was also obtained from the NASA Langley Research Directorate.

## References

- [1] Herring, G.C., Lee, J.W., and Goad, W.K., "Feasibility of Rayleigh Scattering Flow Diagnostics in the National Transonic Facility," NASA TM-2015-218800, 2015.
- [2] Watkins, A. N., Leighty, B. D., Lipford, W. E., Oglesby, D. M., Goodman, K. Z., Goad, W. K., Goad, L. R., and Massey, E. A. "The Development and Implementation of a Cryogenic Pressure Sensitive Paint System in the National Transonic Facility," 47th AIAA Aerospace Sciences Meeting including The New Horizons Forum and Aerospace Exposition, Orlando, FL, 2009.
- [3] Burner, A., Goad, W., Massey, E., Goad, L., Goodliff, S., and Bissett, O., "Wing Deformation Measurements of the DLR-F6 Transport Configuration in the National Transonic Facility (Invited)", 26th AIAA Applied Aerodynamics Conference, Guidance, Navigation, and Control and Co-located Conferences, (2008)
- [4] King, R. A., Andino, M. Y., Melton, L., Eppink, J., and Kegerise, M. A., "Flow Disturbance Measurements in the National Transonic Facility", AIAA Journal, Vol. 52, No. 1 (2014), pp. 116-130.
- [5] Michael, J. B., Edwards, M. R., Dogariu, A., and Miles, R. B., "Femtosecond Laser Electronic Excitation Tagging for Quantitative Velocity Imaging in Air," Applied Optics, Vol. 50, No. 26, 2011, pp. 5158–5162.
- [6] Burns, R. A., Danehy, P. M., Halls, B. R., and Jiang, N., "Femtosecond Laser Electronic Excitation Tagging Velocimetry in a Transonic, Cryogenic Wind Tunnel," AIAA Journal, Vol. 55, No. 2, 2017, pp. 680–685. doi:10.2514/1.J055325
- [7] Burns, R. A., Peters, C. J., and Danehy, P. M., "Unseeded velocimetry in nitrogen for high-pressure, cryogenic wind tunnels, part I: femtosecond-laser tagging" *Meas. Sci. Technol.* **29** 115302, 2018
- [8] Burns, R. A., and Danehy, P. M., "Unseeded Velocity Measurements Around a Transonic Airfoil Using Femtosecond Laser Tagging," *AIAA Journal*, Vol. 55, No. 12, (2017), pp. 4142-4154.
- [9] Foster, J. M., and Adcock, J. B., "Users Guide for the National Transonic Facility Research Data System," NASA TM-110242, April 1996.
- [10] Fuller, D. E., "Guide for Users of the National Transonic Facility," NASA TM-83124, July 1981.
- [11] Slipchenko MN, Miller JD, Roy S, Gord JR, Danczyk SA, and Meyer TR, "Quasi-Continuous Burst-Mode Laser for High Speed Planar Imaging" *Optics Letters* 37 (2012) pp. 1346-1348
- [12] Slipchenko MN, Miller JD, Roy S, Gord JR, and Meyer TR, "All-Diode-Pumped Quasi-Continuous Burst-Mode Laser for Extended High-Speed Planar Imaging" *Optics Express* 21 (2013) pp. 681-689
- [13] Slipchenko MN, Miller JD, Roy S, Meyer TR, Mance JG, and Gord JR "100-kHz, 100-ms, 400-J Burst-Mode Laser with

- Dual Wavelength Diode Amplifiers” *Optics Letters* 39 (2014) pp. 4735-4738
- [14] Beresh, S. J., Kearney, S. P., Wagner, J. L., Guildenbecher, D. R., Henfling, J. F., Spillers, R. W., Pruett, B. O. M., Jiang, N., Slipchenko, M. N., Mance, J., and Roy, S., “Pulse-burst PIV in a high-speed wind tunnel,” *Meas. Sci. Technol.* 26, 1–13 (2015)
- [15] Burns, R. A., Danehy, P. M., Jiang, N., Slipchenko, M. N., Felver, J., and Roy, S., “Unseeded velocimetry in nitrogen for high pressure cryogenic wind tunnels: part II. Picosecond-laser tagging” *Meas. Sci. Technol.* 29 115203, 2018